Published May 26, 2014

A negative feedback loop mediated by the Bcl6–cullin 3 complex limits Tfh cell differentiation

Rebecca Mathew,[1,2,3] Ai-ping Mao,[1,2,3] Andrew H. Chiang,[1,4] Clara Bertozzi-Villa,[1,2,3] Jeffrey J. Bunker,[1,2,3] Seth T. Scanlon,[1,2,3] Benjamin D. McDonald,[1,2,3] Michael G. Constantinides,[1,2,3] Kristin Hollister,[5] Jeffrey D. Singer,[6] Alexander L. Dent,[5] Aaron R. Dinner,[1,4] and Albert Bendelac[1,2,3]

[1]Committee on Immunology, [2]Department of Pathology, [3]Howard Hughes Medical Institute, and [4]Department of Chemistry, University of Chicago, Chicago, IL 60637
[5]Department of Microbiology and Immunology, Indiana University School of Medicine, Indianapolis, IN 46202
[6]Biology Department, Portland State University, Portland, OR 97207

Induction of Bcl6 (B cell lymphoma 6) is essential for T follicular helper (Tfh) cell differentiation of antigen-stimulated CD4+ T cells. Intriguingly, we found that Bcl6 was also highly and transiently expressed during the CD4+CD8+ (double positive [DP]) stage of T cell development, in association with the E3 ligase cullin 3 (Cul3), a novel binding partner of Bcl6 which ubiquitinates histone proteins. DP stage–specific deletion of the E3 ligase Cul3, or of Bcl6, induced the derepression of the Bcl6 target genes *Batf* (*basic leucine zipper transcription factor, ATF-like*) and *Bcl6*, in part through epigenetic modifications of CD4+ single-positive thymocytes. Although they maintained an apparently normal phenotype after emigration, they expressed increased amounts of *Batf* and *Bcl6* at basal state and produced explosive and prolonged Tfh responses upon subsequent antigen encounter. Ablation of Cul3 in mature CD4+ splenocytes also resulted in dramatically exaggerated Tfh responses. Thus, although previous studies have emphasized the essential role of Bcl6 in inducing Tfh responses, our findings reveal that Bcl6–Cul3 complexes also provide essential negative feedback regulation during both thymocyte development and T cell activation to restrain excessive Tfh responses.

CORRESPONDENCE
Albert Bendelac:
abendela@bsd.uchicago.edu

Abbreviations used: ChIP, chromatin immunoprecipitation; DP, double positive; GC, germinal center; qRT-PCR, quantitative real-time PCR; RTE, recent thymic emigrant; SAP, SLAM-associated protein; SP, single positive; SSMD, strictly standardized mean difference; Tfh cell, T follicular helper cell; Tg, transgenic.

The transcription factor Bcl6 (B cell lymphoma 6) is rapidly induced upon peripheral activation of CD4+ T cells and plays a central role in the acquisition of the T follicular helper (Tfh) cell program (Crotty, 2011; Nutt and Tarlinton, 2011; Vinuesa and Cyster, 2011; Liu et al., 2013) and in antagonizing other T effector programs (Nurieva et al., 2009; Choi et al., 2011; Nakayamada et al., 2011; Pepper et al., 2011). Recent studies have identified Batf (basic leucine zipper transcription factor, ATF-like), an AP-1 factor, as a critical determinant of Bcl6 induction and a global regulator of the Tfh program (Betz et al., 2010; Ise et al., 2011). Thus, Batf binds and activates the promoter of Bcl-6, as well as several other key Tfh genes, including *cMaf* and *Il21*, and Tfh development is severely impaired in its absence. Batf is also a global regulator of the RORγt-driven Th17 cell differentiation (Schraml et al., 2009), which Bcl6 inhibits (Nurieva et al., 2009; Yu et al., 2009; Lu et al., 2011). Recent studies demonstrated that Batf binds cooperatively with Irf4 to composite genomic sequences found in the regulatory regions of multiple genes involved in Tfh, Th17, and Th2 programs, highlighting the central importance of these factors in the emergence of effector programs (Ciofani et al., 2012; Glasmacher et al., 2012; Li et al., 2012; Tussiwand et al., 2012).

Intriguingly, both RORγt and Bcl6 are transiently expressed during T cell development at the CD4+CD8+ double-positive (DP) stage (Sun et al., 2000; Hyjek et al., 2001). Although RORγt is essential to prolong the lifespan of DP thymocytes as they undergo successive rearrangements of their TCR α locus (Guo et al.,

The Rockefeller University Press $30.00
J. Exp. Med. 2014 Vol. 211 No. 6 1137-1151
www.jem.org/cgi/doi/10.1084/jem.20132267

Published May 26, 2014

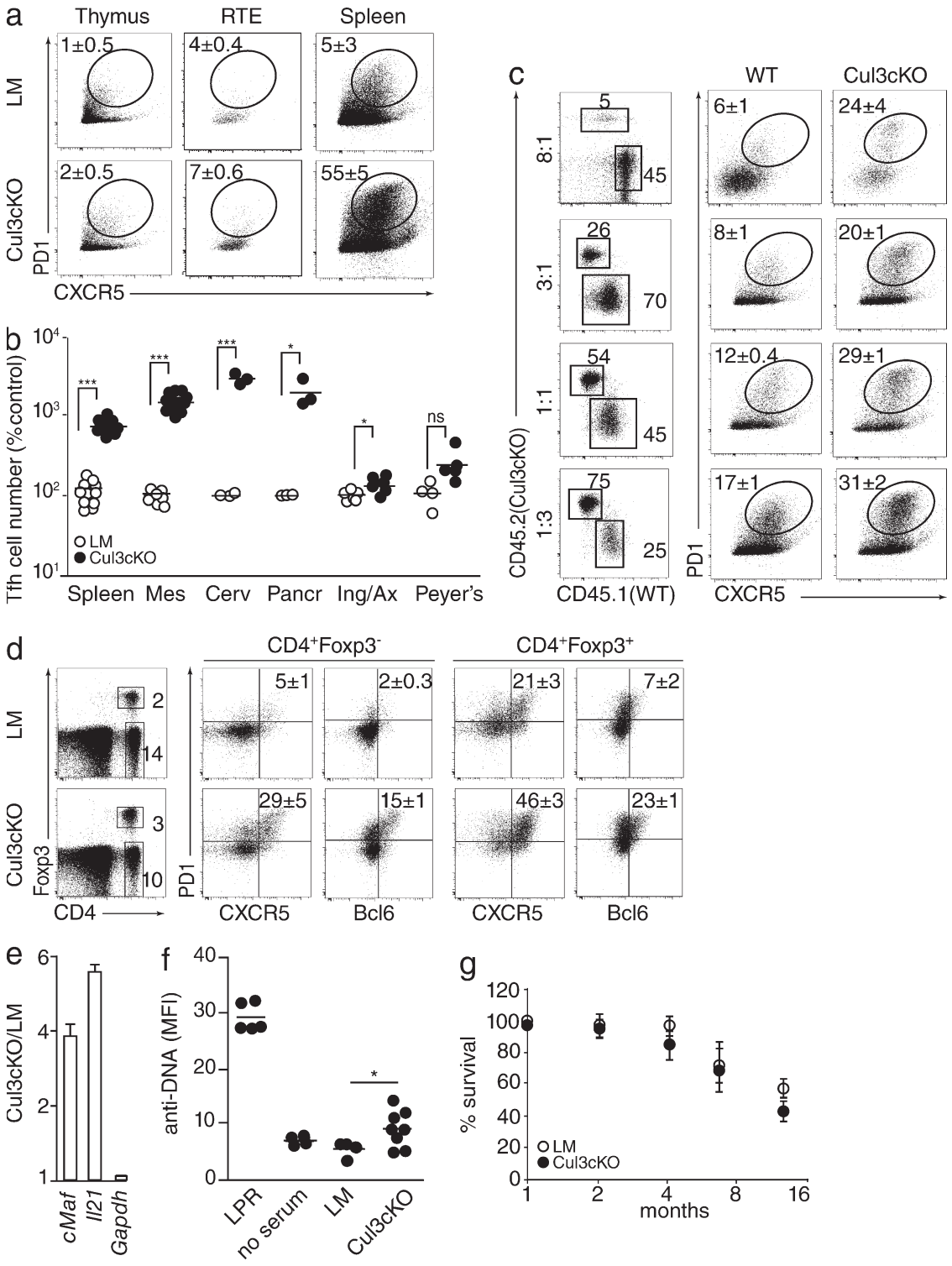

Figure 1. Excessive Tfh formation in *Cul3*$^{fl/fl}$ *Cd4-cre* mice. (a) FACS analysis of thymic CD4+ SP, RTEs, and splenic CD4+ in 10–15-wk-old Cul3cKO and littermate (LM) controls. Numbers indicate percentage (mean ± SEM) of CXCR5+PD1+ Tfh cells among two to eight mice/group from two to four independent experiments. (b) Tfh cell numbers in 16-wk-old Cul3cKO and littermate control splenic, mesenteric, cervical, and pancreatic lymph nodes, inguinal/axillary lymph nodes, and Peyer's patches. Data are a compilation of two to six independent experiments with a total of 3–11 mice. (c) Mixed bone marrow chimeras reconstituted with various KO/WT bone marrow cell ratios analyzed for Tfh frequency 10 wk after reconstitution. Data are representative of two to three mixed chimeras per group from two independent experiments. (d) FACS analysis of splenic CD4+ Tfh, T reg, and Tfr cells from 9-wk-old Cul3cKO and littermate control mice. The leftmost column shows the gating strategy for CD4+Foxp3− and CD4+Foxp3+ cells. Data represent two independent experiments with a total of three mice each examined. Values represent the percentage of cells (mean ± SEM). (e) qRT-PCR analysis of *cMaf* and *Il21* in splenic CD4+ T cells (sorted as CD4+CD25−CD1d-PBS57-tetramer−)

Published May 26, 2014

2002), there is currently no thymic function assigned to Bcl6. Bcl6 is a BTB-ZF transcription factor that can recruit corepressor and coactivator complexes to establish epigenetic marks at target genes (Basso and Dalla-Favera, 2012). Thus, thymic expression of Bcl6, even transient, might induce lasting changes in T cells emerging from development.

We recently identified cullin 3 (Cul3), an E3 ubiquitin ligase known to use BTB proteins as adaptors for substrate recognition, as a component of the transcriptional complex associated with the NKT lineage–specific BTB-ZF transcription factor PLZF (Mathew et al., 2012). Cul3 induced the ubiquitination of histones and of the genome organizers SATB1 and lamin B1, suggesting regulation at the chromatin level. Conditional ablation of Cul3 in *Cd4-cre*$^{+/-}$*Cul3*$^{fl/fl}$ (Cul3cKO) mice led to a block in NKT thymic development similar to the PLZF-null mutation. Intriguingly, the mutant mice also exhibited a spontaneous increase in the frequency of Tfh and germinal center (GC) B cells in peripheral tissues (Mathew et al., 2012). Here, we identified a negative feedback loop whereby Bcl6–Cul3 complexes repressed *Batf* and *Bcl6* during thymic development. This thymic regulation was associated with lasting repressive epigenetic marks that limited the Tfh potential of mature CD4$^+$ T cells upon subsequent encounter with antigen in peripheral lymphoid tissues. A similar negative autoregulatory feedback operated in peripheral CD4$^+$ T cells because deletion of Cul3 in mature T cells also unleashed exaggerated Tfh responses to antigen. Thus, although previous studies have emphasized the essential role of Bcl6 in inducing Tfh responses (Crotty, 2011; Nutt and Tarlinton, 2011; Vinuesa and Cyster, 2011; Liu et al., 2013), our experiments have uncovered an essential negative autoregulation of the Tfh program exerted by Bcl6–Cul3 complexes and revealed its unexpected importance as early as in thymic development.

RESULTS

Spontaneous Tfh expansion in Cul3-deficient mice

Cul3cKO mice show spontaneous enlargement of secondary lymphoid tissues because of the selective accumulation of Tfh cells and the resulting expansion of GC B cells, whereas other T helper responses are unaffected (Mathew et al., 2012). We found that the Tfh phenotype was not observed in thymic CD4$^+$ single-positive (SP) cells or in recent thymic emigrants (RTEs) but developed progressively in the spleen and in mesenteric, cervical, and pancreatic lymph nodes, whereas axillary/inguinal lymph nodes and Peyer's patches were much less affected (Fig. 1, a and b). Interestingly, although the Tfh expansion was mostly made of conventional CD4$^+$ T cells, it also included Foxp3$^+$ T follicular regulatory (Tfr) cells (Fig. 1 d). In lethally irradiated mice reconstituted with CD45 congenic mixtures of WT and KO bone marrows, the T cell defect was

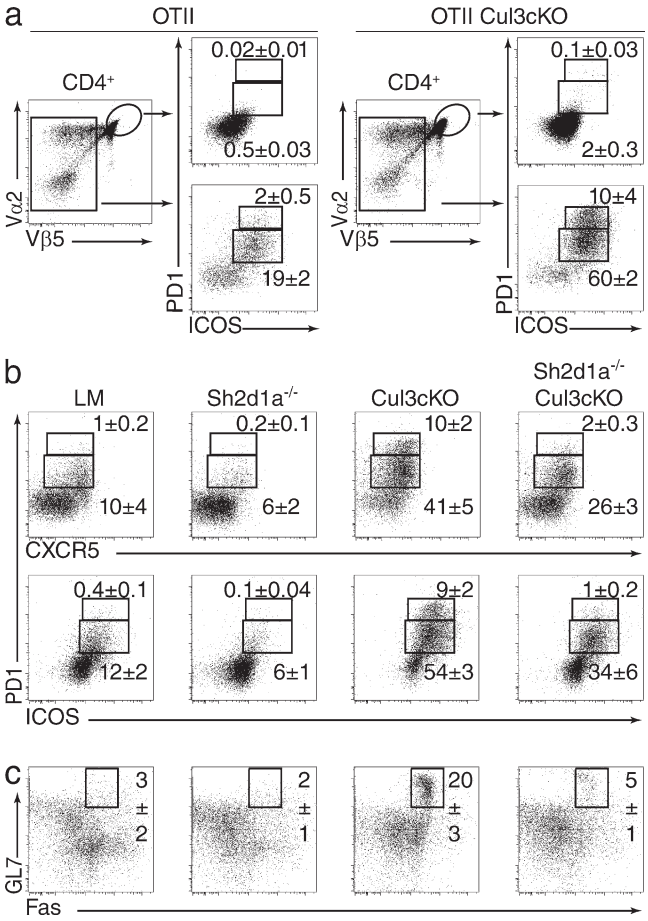

Figure 2. TCR- and SAP-dependent Tfh formation. (a) FACS analysis of splenic CD4$^+$ T cells from 10-wk-old OTII Tg with intact or deleted Cul3 as indicated. CD4$^+$ cells gated as TCR Tg$^+$ or TCR Tg$^-$ were stained for ICOS and PD1 to measure the frequency of Tfh cells. Numbers represent mean ± SEM of five mice per group from two independent experiments. (b) FACS analysis of gated CD4$^+$ splenocytes from 10–15-wk-old littermate (LM) controls, Sh2d1a (SAP)$^{-/-}$, Cul3cKO, and Sh2d1a$^{-/-}$ Cul3cKO mice, stained for PD1 and CXCR5 (top) or PD1 and ICOS (bottom). (c) FACS analysis of the same spleens as in b, gated on B220$^+$IgD$^-$ cells to identify GC B cells. Numbers represent the percentage (mean ± SEM) of five mice/group from three independent experiments in corresponding gates. For CD4$^+$ T cells, GC-Tfh cells are identified as PD1^{hi}ICOS^{hi}CXCR5^{hi} and pre-Tfh cells as intermediate for the same markers as shown.

clearly cell intrinsic, but a modest Tfh conversion of WT cells could also be observed at high KO/WT ratio (Fig. 1 c), suggesting some bystander effect, perhaps caused by increased expression of the Tfh-promoting factors *cMaf* and *Il21* (Fig. 1 e).

The Tfh and GC B cell expansions developed progressively over the normal lifespan of Cul3cKO mice, with only slightly increased antinuclear antibodies detected in old age,

from unimmunized 6–8-wk-old mice shown as the ratio of Cul3cKO/littermate control (n = 5 for each group from three independent experiments; mean ± SEM). (f) Hep-2 antinuclear antibodies quantified as mean nuclear fluorescence intensity at 1:40 dilution of sera from 30–50-wk-old Cul3cKO (seven females and one male) and WT littermates (four females), along with a positive control serum from MRL$^{lpr/lpr}$ and a no-serum negative control. (b and f) Horizontal bars indicate mean. (g) Survival curves of cohorts of Cul3cKO mice (n = 21) and WT littermates (n = 19; mean ± SEM). *, P < 0.05; ***, P < 0.001.

Published May 26, 2014

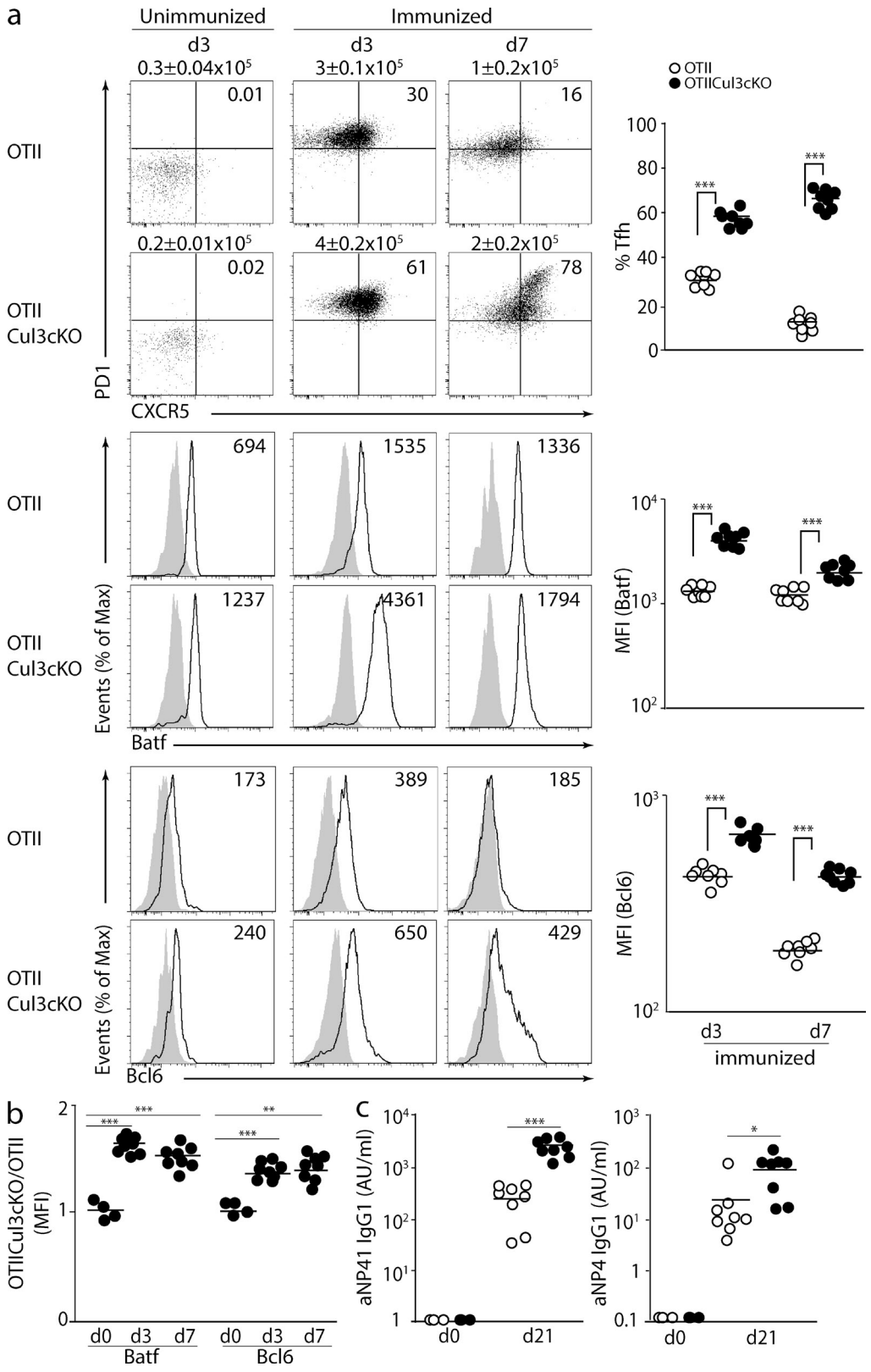

Figure 3. Exaggerated Tfh responses to OVA antigen. (a and b) 0.5 × 10^6 $CD4^+$ enriched SP thymocytes from OTII Tg or OTII Tg Cul3cKO donors were injected i.v. into CD45 congenic recipients 24 h before i.p. immunization with OVA + alum (a) or OVA-NP_{16} + alum (b). (a) Unimmunized controls are shown at day 3 after transfer in the first column, and immunized mice are shown at days 3 and 7 in the second and third columns. Summary data were compiled from two separate experiments, each with four to five mice per group, and statistical analyses are shown on the right. FACS analysis

Published May 26, 2014

but without overt disease or notable anomalies in blood cell counts or in function and histology of lung, liver, and kidney (Fig. 1, f and g; and not depicted). Altogether, the general picture was suggestive of exaggerated Tfh responses to environmental antigens at mucosal surfaces, without overt immunopathological consequences in the B6 background.

Tfh expansion is antigen driven and SLAM-associated protein (SAP) dependent

To test whether the Tfh expansion was dependent on antigen stimulation, we crossed the Cul3cKO mice to OTII TCR transgenic (Tg) mice. As shown in Fig. 2 a, a Tfh expansion still occurred in TCR Tg mice, but it was strictly restricted to the cells that expressed endogenous TCRs ($V\alpha2^{lo}V\beta5^{lo}$), whereas the cells expressing high levels of Tg Vα2 and Vβ5 were not involved. Thus, Tfh expansion depended on TCR specificity.

Tfh cell differentiation occurs in two steps, including a pre-Tfh stage, characterized by intermediate levels of Tfh markers, and a GC-Tfh stage, which depends on SAP-mediated interactions with B cells. Upon deletion of SAP in Cul3-deficient T cells, the expansion of GC-Tfh and GC B cells was markedly decreased (Fig. 2, b and c). However, the pre-Tfh population was still expanded. Thus, Cul3-deficient Tfh cells differentiated along the classical SAP-independent pre-Tfh and SAP-dependent GC-Tfh stages, and their expansion was initiated before GC entry.

Dysregulation of Tfh-inducing transcription factors before antigen encounter and exaggerated Tfh responses after immunization

We transferred 0.5×10^6 WT or Cul3cKO $CD4^+$ enriched SP OTII thymocytes i.v. into unirradiated CD45 congenic recipients to study their response after immunization with cognate antigen OVA in alum. First, we followed unimmunized recipients. Surprisingly, we noted that, although both $CD4^+$ SP thymocytes and 24-h RTEs in Cul3cKO mice failed to express CXCR5 (chemokine [C-X-C motif] receptor 5) and other surface Tfh markers (Fig. 1 a), the transferred cells expressed conspicuously higher amounts of basal Batf (67%) and Bcl6 (41%) on average than their WT counterparts 3 d after transfer, as measured by intracellular flow cytometry (Fig. 3, a [left column] and b). These increased basal levels were maintained without further increase at day 7 after transfer (Fig. 3 b). However, these changes were not sufficient to induce the acquisition of the stereotypical Tfh phenotype because levels of CXCR5, PD1 (programmed cell death 1), and ICOS were not detectably increased in the absence of immunization. Thus, *Cul3* ablation at the DP stage resulted in delayed but stable increases of basal Batf and Bcl6 proteins, without overt Tfh transformation, suggesting that some degree of Tfh dysregulation was already present before antigen exposure.

After immunization, $PD1^{hi}CXCR5^{hi}$ Cul3cKO Tfh cells appeared earlier, expanded faster, and were maintained longer than WT Tfh cells (Fig. 3 a, top two rows). As soon as day 3 after immunization, 62 ± 2% of Cul3cKO cells expressed very high levels of PD1 and CXCR5 compared with only 33 ± 3% of WT. A similar increase was noted for ICOS, GL7, BTLA, and OX40 (not depicted). At day 7, when WT cells were already losing their Tfh phenotype, Cul3cKO cells kept expressing even higher levels of the Tfh markers, reaching 72 ± 5% compared with 13 ± 6% for controls. These differences were confirmed in multiple independent experiments and were highly significant ($P < 0.001$). This exaggerated Tfh response was associated with a rise of Batf and Bcl6 detected by intracellular flow cytometry, which occurred earlier and reached higher and more sustained levels than WT cells (Fig. 3 a, bottom four rows). Importantly, after immunization with OVA-NP_{16} mixed with alum, the Cul3cKO OTII cells drove correspondingly higher titers of anti-NP antibodies detected by ELISA with BSA-NP_{41}, as well as high-affinity antibodies detected with BSA-NP_4, indicating normal Tfh functions (Fig. 3 c).

The exaggerated Tfh response was associated with increased expression of Ki67, suggesting markedly increased proliferation of Cul3cKO Tfh cells (Fig. 4 a, second row). It did not appear to occur at the expenses of other T helper programs because Cul3cKO mice immunized with OVA mixed with alum or with OVA mixed with CFA exhibited the same bias toward $Gata3^+$ Th2 cells or $Tbet^+$ Th1 cells, respectively (Fig. 4, a and b). Altogether, these results indicated that although Cul3cKO $CD4^+$ T cells exhibited baseline increases in Batf and Bcl6 after exiting the thymus, they acquired their exaggerated Tfh cell differentiation after immunization in the periphery.

Altered Tfh gene expression in Cul3-deficient thymocytes

The stable baseline increase of Batf and Bcl6 proteins observed shortly after thymic maturation of Cul3cKO $CD4^+$ T cells suggested that fresh thymocytes might already express detectable changes at the transcriptional level. Using quantitative real-time PCR (qRT-PCR), we measured the *Batf* transcript levels in large and small DP thymocytes, as well as in $CD4^+$ SP thymocytes. Fig. 5 a shows that although *Batf* transcripts were not

shows staining of gated donor cells in the spleen for PD1 and CXCR5 (top two rows), Batf (middle two rows), Bcl6 (bottom two rows). Numbers above panels in the top two rows represent absolute numbers of donor cells recovered in the recipient spleens (mean ± SEM), with the percentage of $PD1^{hi}CXCR5^{hi}$ cells indicated in the top right quadrant of each dot plot. In the bottom four rows, numbers represent mean fluorescence intensity (MFI), with shaded gray histograms representing background staining. (b) Comparative levels of Batf and Bcl6 proteins (expressed as OTII Cul3cKO/WT MFI ratio) in $CD4^+$ SP thymocytes before (day 0) and after parking for 3 and 7 d (in vivo transfer) in individual unimmunized mice. Data are combined from two independent experiments with four to eight mice in each group. (c) Serum IgG1 antibodies against BSA-NP_{41} (left) and BSA-NP_4 (right) at days 0 and 21 after immunization with OVA-NP_{16} + alum. Data are a compilation of two independent experiments, with a total of eight immunized mice in each group. Horizontal bars indicate mean. *, $P < 0.05$; **, $P < 0.01$; ***, $P < 0.001$.

Published May 26, 2014

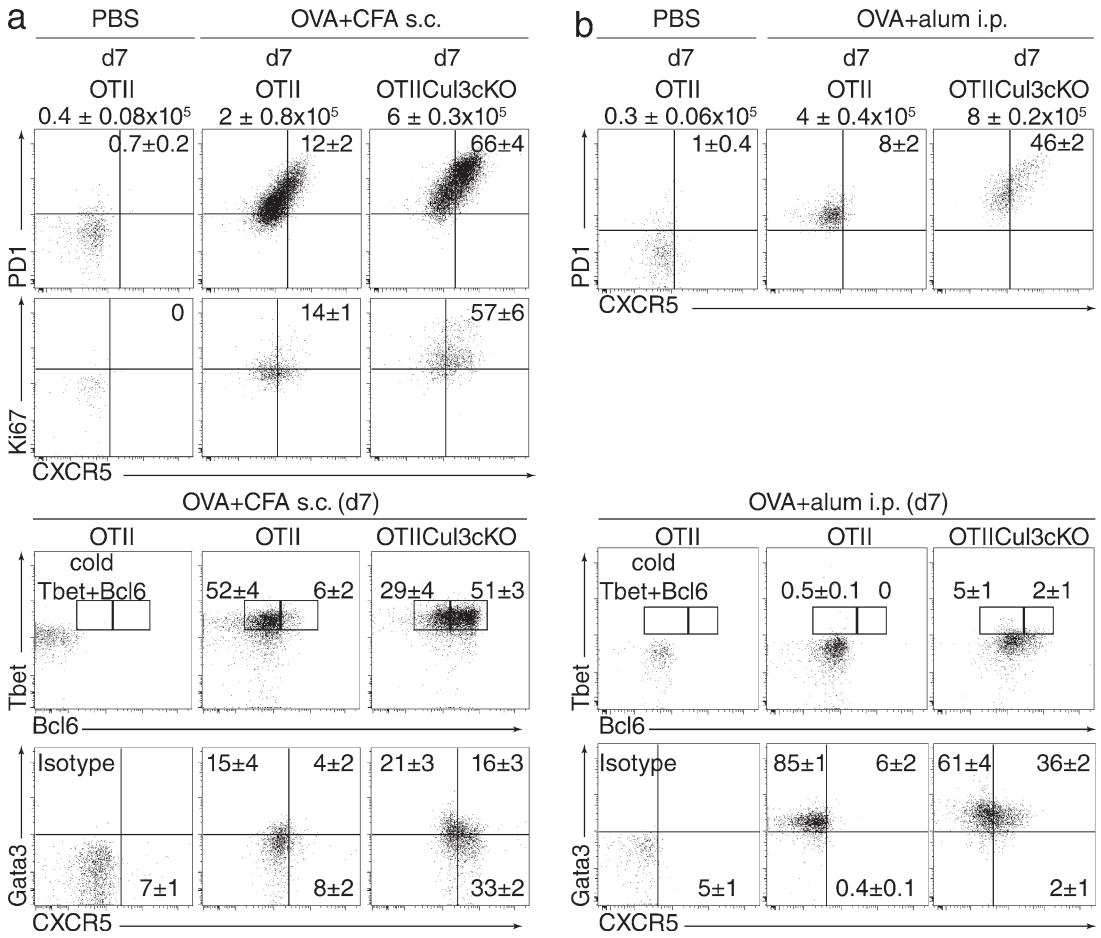

Figure 4. Exaggerated Tfh responses without alteration of Th1 or Th2 programs. (a and b) 0.5 × 10^6 $CD4^+$ enriched SP thymocytes from OTII or OTII Cul3cKO donors were injected i.v. into CD45 congenic recipients 24 h before injection of OVA + CFA s.c., OVA + alum i.p., or PBS, as indicated. OTII cells were analyzed at day 7 after immunization in inguinal lymph nodes (CFA; a) or spleen (alum; b). (first row) Expression of CXCR5 and PD1. Numbers above the dot plots are the absolute numbers of OTII cells recovered from the lymph nodes or spleen. Numbers in top right quadrants are the percentage of $CXCR5^+PD1^+$ (mean ± SEM). (second row) Expression of Ki67 and CXCR5. (third row) Expression of Tbet and Bcl6. Numbers indicate the percentage (mean ± SEM) of $Tbet^{hi}Bcl6^{hi}$ cells (right box) or $Tbet^{hi}Bcl6^{int}$ cells (left box). Background staining is shown after preincubation with an excess of unconjugated antibodies (cold Tbet+Bcl6). (fourth row) Expression of Gata3 and CXCR5 with quadrant statistics (mean ± SEM). Background staining is shown for fluorochrome-conjugated isotype control. Data are representative of two independent experiments with total $n = 6$ mice.

quantitatively altered at the early, large-DP stage in Cul3cKO mice, they were already significantly increased at the small-DP stage compared with littermate controls and further elevated at the SP stage. This kinetics was consistent with the genetic ablation of *Cul3* at the early DP stage by the *Cd4-Cre* transgene. Thus, although increased Batf protein was detected soon after thymic emigration at the single cell level, transcriptional changes were already evident at the DP stage immediately after Cul3 ablation. A similar picture was noted for *Bcl6*, which was expressed at a higher level in Cul3cKO than in WT $CD4^+$ SP thymocytes (Fig. 5 b). Importantly, these alterations were cell intrinsic, as the analysis included several mixed (1:1) bone marrow chimeras in which Cul3cKO and WT $CD4^+$ SP thymocytes could be compared side by side.

We performed a comparative whole genome microarray analysis of $CD4^+$ SP thymocytes in WT and Cu3-deficient littermates and examined a larger Tfh set of 14 genes, defined based on previously published work (Vinuesa et al., 2005; Nurieva et al., 2008; Yusuf et al., 2010), which included *Slamf6*, *Il21*, *Cxcr5*, *Maf*, *Icos*, *Irf4*, *Batf*, *Bcl6*, *Pdcd1*, *Sh2d1a*, *Tiam1*, *Stat4*, *Tnfsf11*, and *Cd44*. By examining gene resolution fold changes of Cul3cKO over WT with biological replicates plotted as x and y axes, we found that Tfh genes were particularly up-regulated relative to other genome-wide changes in expression (Fig. 5 c). The Tfh-specific up-regulation was highly significant, as shown by comparing the Tfh gene set with randomly generated sets of genes using Monte Carlo–generated simulations ($P = 2 \times 10^{-6}$). In contrast, a similar analysis of the Th1 and Th2 gene sets (detailed in the Materials and methods section) failed to show significant enrichment in Cul3cKO compared with WT $CD4^+$ SP thymocytes, confirming the Tfh-specific nature of the thymic changes.

Published May 26, 2014

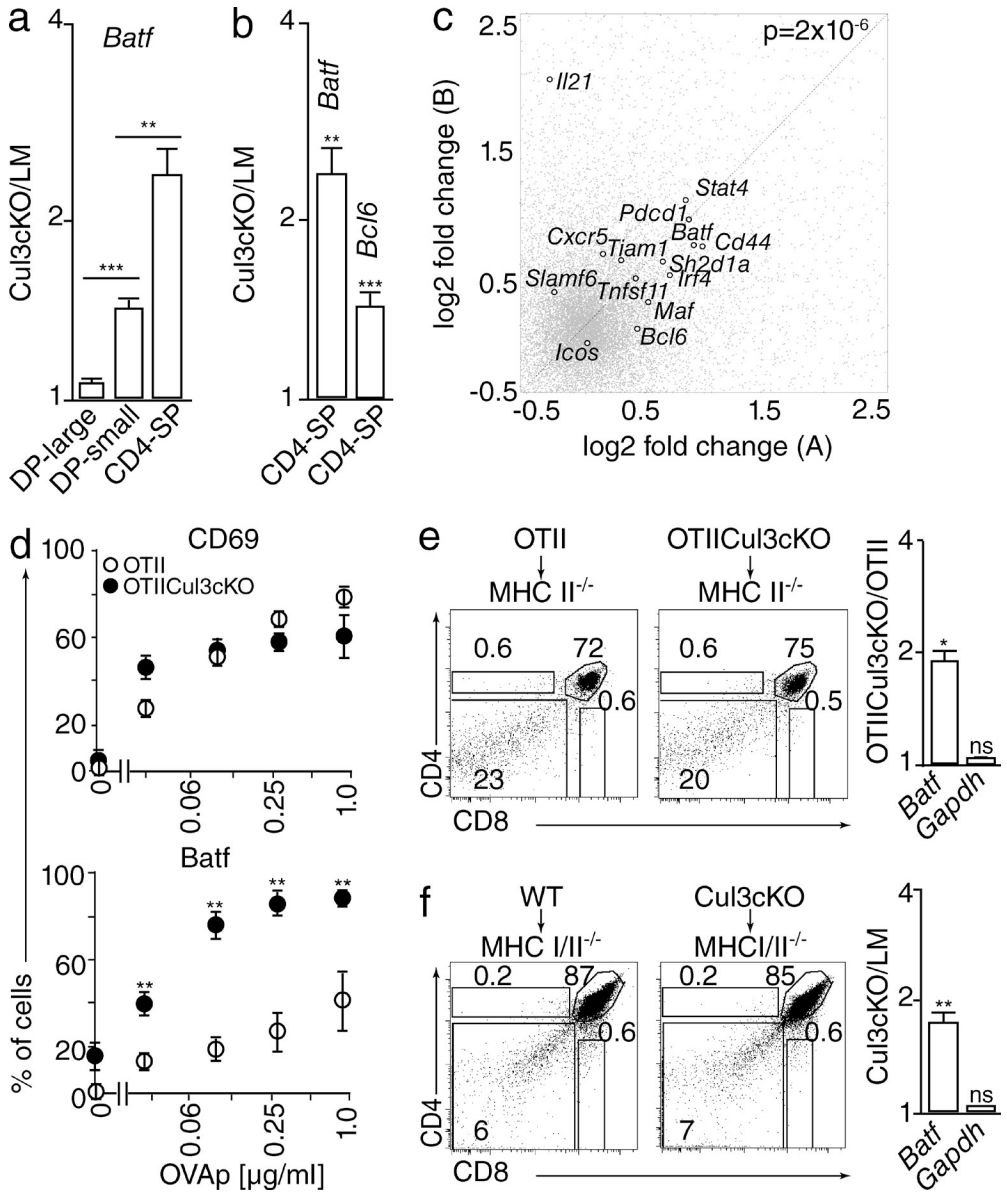

Figure 5. Altered Tfh gene expression in Cul3-deficient thymocytes. (a) qRT-PCR analysis of *Batf* in large DP, small DP, and CD4+ SP thymocytes shown as ratio of Cul3cKO/littermate (LM) control. (b) qRT-PCR analysis of *Batf* and *Bcl6* in CD4+ SP thymocytes shown as ratio of Cul3cKO/littermate control. Bar graphs represent mean ± SEM from 5–10 pairs of KO and controls from five independent experiments. (c) Gene resolution fold changes of CD4+ SP thymocyte microarrays in Cul3cKO versus littermate controls, with biological replicates plotted as x- and y-axis coordinates. The Tfh gene set, indicated as large black scatter, is significantly up-regulated relative to other genome-wide changes in expression, as shown by comparative SSMD analysis of Monte Carlo–generated sets ($P = 2 \times 10^{-6}$). In contrast, the Th1 and Th2 gene sets (not indicated in the figure) were not significantly altered (P = 0.3). (d) CD69-MACS–depleted OTII Tg thymocytes were stimulated with T cell–depleted CD45 congenic splenic APCs at different concentrations of OVA peptide for 20 h before FACS analysis of CD4+ SP cells for surface CD69 and intracellular Batf. Mean ± SEM of two independent experiments with three WT and three Cul3cKO is shown. (e) MHC II–deficient hosts were lethally irradiated and reconstituted with bone marrow cells from OTII Tg in a Cul3cKO or WT background as indicated. CD4/CD8 dot plots show absence of SP thymocytes at 5–6 wk after reconstitution, as expected. Bar graph shows Batf expression measured by qRT-PCR as a ratio of Cul3cKO/WT purified small DP thymocytes (mean ± SEM). Data are compiled from three WT and six KO from two independent experiments. (f) Same experiment as in panel e for MHC I/II double-deficient hosts reconstituted with Cul3cKO or WT bone marrow cells as indicated. Data are compiled from three WT and three KO from one experiment. *, P < 0.05; **, P < 0.01; ***, P < 0.001.

TCR-independent up-regulation of Batf

Recent studies suggested a potential correlation between strength of TCR signaling and Tfh responses (Fazilleau et al., 2009; Tubo et al., 2013). When stimulated in vitro with APC and peptide, Cul3cKO CD4+ SP OTII thymocytes exhibited a massive increase of Batf, compared with WT cells, over a large range of peptide antigen concentrations, but, importantly, other proteins induced by TCR signaling

Published May 26, 2014

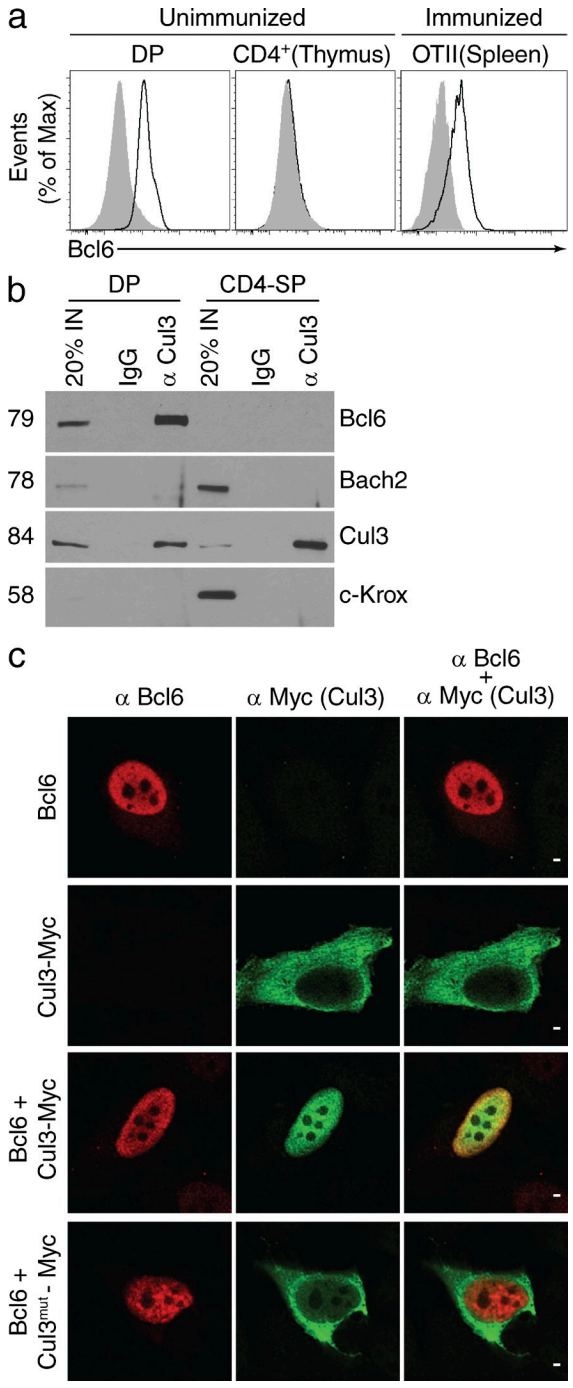

Figure 6. Bcl6 interaction with Cul3 in thymocytes. (a) Intracellular staining of Bcl6 in unimmunized $CD4^+8^+$ (DP) and $CD4^+$ SP thymocytes and in splenic $CD4^+$ OTII Tg cells transferred into naive recipients and immunized with OVA 3 d before analysis. Data are representative of two to three independent experiments with two to three mice per group. (b) Immunoprecipitation and Western blot analysis of lysates from fresh DP or $CD4^+$ SP thymocyte (20×10^6 per immunoprecipitation), as indicated. Data are representative of two independent experiments. Molecular mass is indicated in kilodaltons. IN, input lysate. (c) Confocal microscopic analysis of Bcl6 and Cul3 in transfected HeLa cells, as indicated. Cul3mut has the double mutation (L52AE55A) abolishing binding to BTB domains. Data are representative of two independent experiments. Bars, 1 µm.

such as CD69 were at similar levels, indicating the specific nature of Batf dysregulation and the absence of global alteration of TCR signaling (Fig. 5 d). We also asked whether the Tfh bias might be dependent on TCR signaling events during thymic development. We transplanted bone marrow from OTII Tg mice with a WT or Cul3cKO background into lethally irradiated MHC II–deficient hosts. Although, as expected, the TCR Tg thymocytes did not progress beyond the DP stage in these chimeras because of lack of positive selection, Fig. 5 e shows that Cul3cKO DP thymocytes did up-regulate *Batf* transcripts (compared with WT DP) in the MHC II–deficient background as well, indicating that the up-regulation was independent of TCR engagement. A similar conclusion was derived from the analysis of unselected DP thymocytes obtained from MHC I/II double KO irradiated recipients reconstituted with WT or Cul3cKO bone marrow (Fig. 5 f). Thus, the basal up-regulation of *Batf* transcript observed in thymocytes lacking Cul3 did not depend on TCR signaling.

Bcl6–Cul3 complexes in fresh thymocytes

Human cortical thymocytes were previously shown to express the Bcl6 protein (Hyjek et al., 2001), and their mouse counterparts transiently express *Bcl6* mRNA at the DP stage according to a public database (ImmGen). Flow cytometric analysis of WT mouse thymocytes revealed high amounts of Bcl6 in DP thymocytes and rapid down-regulation in SP cells (Fig. 6 a). Notably, the thymic expression levels were comparable or superior to those elicited after immunization in peripheral Tfh cells.

Immunoprecipitation of Cul3 followed by Western blot analysis of fresh DP thymocytes demonstrated that >20% of Bcl6 was bound to Cul3 (Fig. 6 b). Other BTB-ZF transcription factors such as Bach2 and c-Krox, which are expressed later at the SP stage, were not coprecipitated by anti-Cul3 antibodies in SP cells. The binding of Bcl6 to Cul3 was further confirmed by transfection in HeLa cells (Fig. 6 c). Although single transfection experiments in HeLa cells showed that Bcl6 located to the nucleus and Cul3 was mainly found in the cytosol, cotransfection resulted in the transport of Cul3 to the nucleus. Furthermore, nuclear transport depended on the Cul3 residues L52 and E55, which were previously shown to be specifically involved in binding BTB proteins (Fig. 6 c, bottom row; Wimuttisuk and Singer, 2007). Altogether, these results indicated that Bcl6 protein was naturally and transiently expressed in mouse DP thymocytes where it was prominently associated with Cul3.

Bcl6 binds and regulates the *Batf* promoter in thymocytes

As Batf was recently shown to be a key inducer of several Tfh genes, including *Bcl6*, *cMaf*, and *Il21* (Ise et al., 2011), the simplest hypothesis explaining the above observations was that Bcl6–Cul3 complexes exerted a negative feedback on the Tfh program by repressing *Batf* and *Bcl6*. Recent chromatin immunoprecipitation (ChIP)–Seq studies of Bcl6-expressing macrophages identified Bcl6 binding to the first intron of the *Batf*

Published May 26, 2014

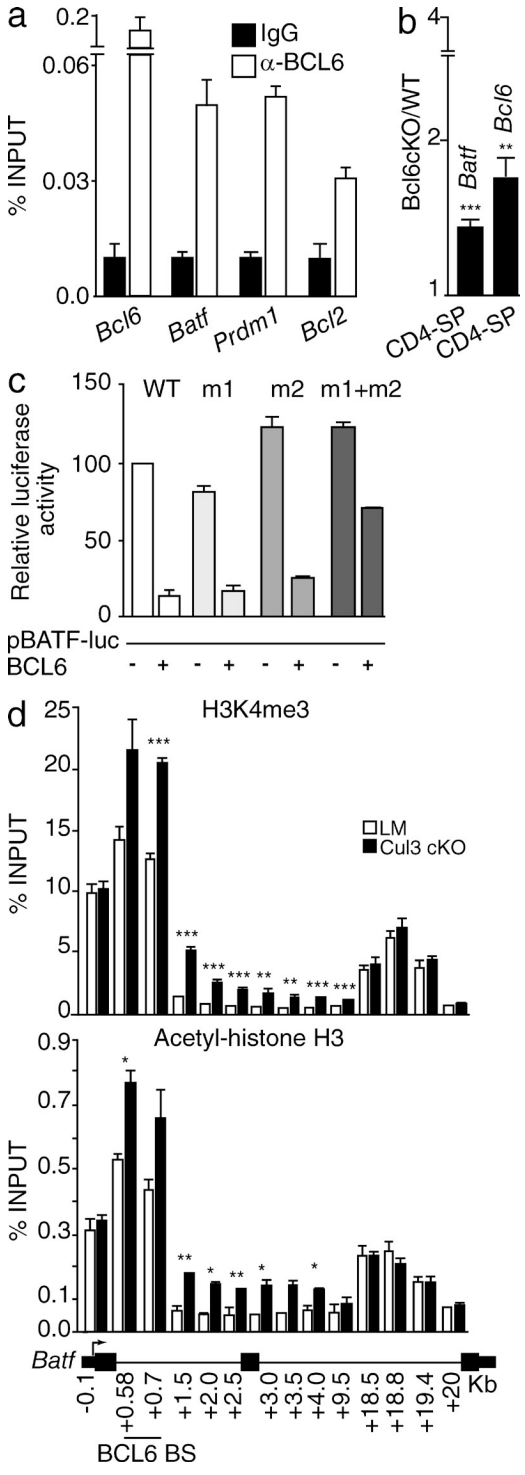

Figure 7. The Bcl6–Cul3 complex directly regulates *Batf* and *Bcl6*. (a) ChIP-qPCR analysis of Bcl6 binding to the indicated genes in fresh thymocytes. Data are representative of two independent experiments (mean ± SEM). (b) qRT-PCR analysis of *Batf* and of *Bcl6* (exons 2–3) in exon 7–9–deleted Bcl6cKO versus WT CD4+ SP thymocytes. Bar graphs represent mean ± SEM from five pairs of KO and controls from two independent experiments. (c) Transfection of Bcl6 together with luciferase-based reporters of Batf in HeLa cells. Mutated intronic regulatory sequences (m1 and m2) are as indicated. Bar graphs represent mean ± SEM from two independent experiments. (d) ChIP-qPCR analysis of H3K4me3 and acetyl-H3 along the *Batf* gene (indicated at bottom) in Cul3cKO versus littermate (LM) control CD4+ SP thymocytes. Bcl6-binding sequences are at 0.58 and 0.7 kb in the first intron. Data are representative of two independent experiments (mean ± SEM). *, $P < 0.05$; **, $P < 0.01$; ***, $P < 0.001$.

gene, which contains a putative Bcl6-binding sequence motif (Barish et al., 2010, 2012). Using ChIP-qPCR, we demonstrated direct binding of Bcl6 to this intronic region of *Batf* in fresh thymocytes (Fig. 7 a). We also detected binding of Bcl6 to the *Bcl6* proximal promoter, which includes a binding site previously identified in B cell lymphoma cells (Wang et al., 2002; Pasqualucci et al., 2003), as well as to *Prdm1* and *Bcl2* (Parekh et al., 2007). Thus, these findings demonstrated that, despite its transient expression, Bcl6 protein did bind key regulatory elements of multiple genes in fresh DP thymocytes.

Notably, *Batf* transcripts were significantly up-regulated in Bcl6cKO CD4+ SP thymocytes, supporting the conclusion that Bcl6 and Cul3 together regulate *Batf* during thymic development (Fig. 7 b). Furthermore, we detected a significant increase in the mRNA segment encompassing the exon 2–3 junction of *Bcl6* in exon 7–9–deleted Bcl6cKO compared with WT (Fig. 7 b). These findings are consistent with an inhibitory function of Bcl6 on the transcription of *Batf* and *Bcl6*.

To further dissect how Bcl6 could regulate the transcription of *Batf*, we cotransfected *Bcl6* along with a luciferase-based *Batf* reporter in HeLa cells (Fig. 7 c). The pBATF-luc plasmid alone was strongly repressed in cells cotransfected with Bcl6. As there were at least two potential binding sites for Bcl6 in the first intron of *Batf* based on sequence analysis, we examined the effects of individual and double mutations at these sites. Only the double mutation significantly relieved the repression mediated by Bcl6, suggesting that the two binding sites were used in vivo. Altogether, these results indicated that Bcl6 could directly bind regulatory elements repressing *Batf* transcription in thymocytes.

Cul3-dependent epigenetic changes in the *Batf* gene

Because the up-regulation of *Batf* mRNA begins in Cul3cKO DP thymocytes and persists after emigration to the periphery, at a time when there is little residual Bcl6, we examined whether Cul3 might have helped establish lasting epigenetic marks in the *Batf* gene. A significant increase in H3K4Me3 and H3Ac marks were detected in Cul3cKO CD4+ SP thymocytes, mostly around the first intron region harboring the Bcl6-binding sites (Fig. 7 d). Thus, deletion of Cul3 at the DP stage resulted in altered epigenetic marks at the *Batf* gene in emerging CD4+ T cells.

Cul3 ablation in mature CD4+ T cells

In Cul3cKO mice, the early dysregulation of Tfh-inducing genes in thymocytes preempted the assessment of an additional role of Cul3 during antigen stimulation of mature CD4+ T cells. To test whether a similar autoregulatory feedback existed in

Published May 26, 2014

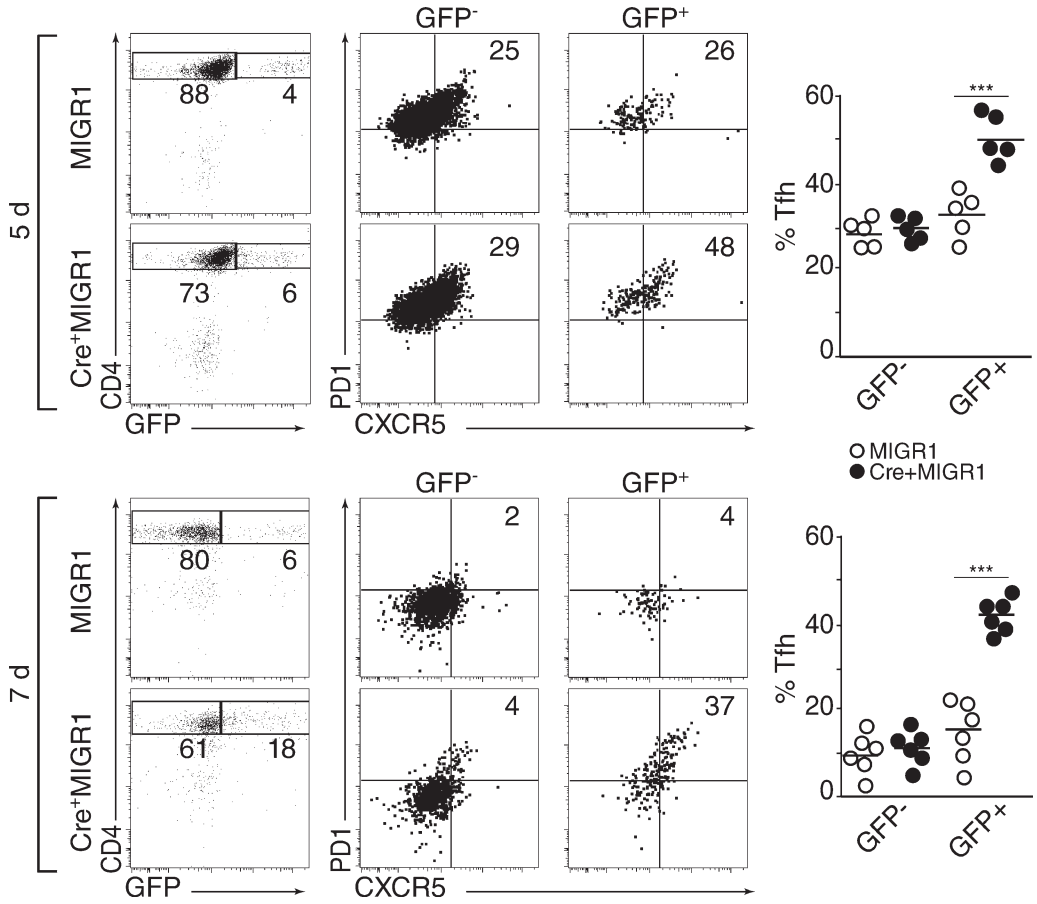

Figure 8. Cul3 regulates Tfh responses in mature CD4+ splenocytes. CD4+ splenocytes from OTII Tg Cul3$^{fl/fl}$ mice were transduced with MIGR1 retrovirus expressing Cre and GFP, or GFP alone, as indicated, and injected into CD45 congenic recipients 24 h before immunization with OVA + alum, as described in Fig. 3. Mice were analyzed 5 and 7 d after immunization, as indicated. The first column shows the fraction of GFP+ cells among donor cells (CD45.2+) at time of recovery. The second and third columns show staining of gated CD4+ donor cells separated according to GFP expression. The fourth column shows summaries of individual data. Numbers represent the percentage of PD1^{hi}CXCR5^{hi} Tfh cells based on three separate experiments for day 5 (n = 5) and day 7 (n = 6). Horizontal bars indicate mean. ***, P < 0.001.

mature CD4+ T cells undergoing Tfh cell differentiation, we deleted Cul3 by retroviral expression of Cre recombinase in Cul3$^{fl/fl}$ OTII Tg CD4+ splenocytes. After transduction, cells were reinjected into naive hosts, which were subsequently immunized with OVA, following the same protocol as in Fig. 3. Fig. 8 shows that the GFP-expressing cells derived after transduction with MIGR1-Cre, but not control MIGR1, also exhibited a highly significant exaggeration of Tfh cell differentiation at various times after immunization (P < 0.001). Thus, we conclude that the Cul3-mediated negative feedback of Tfh cell differentiation also operates in mature CD4+ T cells undergoing antigen stimulation.

DISCUSSION

This study provides several new insights into the regulation of Tfh responses. First, it reveals the exquisite role of Cul3, the E3 ligase which is specifically recruited by Bcl6, in regulating the Tfh transcriptional program of CD4+ T cells. Second, it establishes the existence of a potent negative feedback loop whereby Bcl6–Cul3 complexes can directly repress the key Tfh-inducing genes *Bcl6* and *Batf*. Third, and unexpectedly, it shows that the feedback loop also operates before antigen encounter by epigenetic marking during thymic development.

The BTB domain of the transcription factor Bcl6 homodimerizes to provide a platform that recruits a complex set of proteins with transcriptional regulatory activity. These include the corepressor proteins NCOR and SMRT, which bind in a mutually exclusive manner in a groove formed at the dimer interface, the MTA3 subunit of the nucleosome remodeling and deacetylase complex, the DNA methyltransferase DNMT1, the histone deacetylase HDAC1, and Polycomb group proteins (Basso and Dalla-Favera, 2012). Cul3 is known to directly bind BTB proteins and use them as adaptors for substrate recognition and ubiquitination (Duda et al., 2011; Errington et al., 2012). In a previous study of PLZF, a BTB-ZF transcription factor which directs NKT lineage cell differentiation, we demonstrated that the targets of ubiquitination included histone proteins and the genome organizers SATB1 and LaminB1, which colocalized with PLZF in the nuclear environment, but not the BTB protein itself (Mathew et al.,

Published May 26, 2014

2012). Thus, Bcl6 is associated with a complex set of partner proteins that can mediate various epigenetic modifications at different target sites, and selective disruptions of these interactions have the potential to reveal novel functions of Bcl6 (Huang et al., 2013).

The conditional ablation of either *Cul3* or *Bcl6* in thymocytes resulted in significant changes of expression of *Batf* and of *Bcl6* itself, revealing a negative feedback loop exerted by Bcl6–Cul3 complexes in thymocytes. This regulation involved the direct binding to, and repression of, *Batf*, a global initiator of the Tfh pathway, which is essential for induction of *Bcl6*, *cMaf*, and *Il21* (Betz et al., 2010; Ise et al., 2011). In addition, as previously reported for B cell lymphomas (Pasqualucci et al., 2003), our studies suggested that, in thymocytes, Bcl6 could also bind and repress its own gene in an autoregulatory loop. Thus, our findings identify a potent negative feedback loop built into the Tfh program, an unusual feature among other T helper effector programs, which generally show self-reinforcement rather than self-limitation. Notably, previous studies demonstrated that Bcl6 could induce several genes associated with the Tfh program, including the endogenous *Bcl6* itself (Nurieva et al., 2009), after overexpression in vitro. Although this study of Bcl6 autoinduction is in apparent conflict with our findings, we note that our results were obtained in vivo and that negative autoregulation of Bcl6 has also been demonstrated in B cells (Pasqualucci et al., 2003). Thus, it is possible that Bcl6 might contribute to both its induction and feedback inhibition, perhaps depending on the stage of the Tfh response, the level of Bcl6 expression, or the changing environment of other transcription factors associated with the Bcl6 network. Although our findings are consistent with the possibility that Cul3 regulated Bcl6 function, for example through the ubiquitination of critical components of the Bcl6 transcriptional complex, as suggested for PLZF (Mathew et al., 2012), the precise nature of these changes and their causal relationship remain elusive. It is also possible that Cul3 directly ubiquitinates Bcl6, thereby altering its function or its lifespan, although we have failed to document such changes so far. In any case, our findings clearly document the key role of Cul3 in regulating the Bcl6-mediated Tfh program, providing an explanation for the exaggerated Tfh responses in the absence of Cul3 in vivo.

It is noteworthy that conditional ablation of Cul3 in B cells resulted in the loss of GC formation (Mathew et al., 2012), whereas ablation in T cells increased Tfh cell differentiation and GC formation. It has been shown that by modulating the DNA damage response and controlling apoptosis, Bcl6 was critical for B cells to tolerate the DNA breaks associated with somatic hypermutation (Parekh et al., 2007). This critical antiapoptotic function of Bcl6 in GC B cells might explain why the absence of Cul3 has such drastic consequences. Interestingly, mice engineered to express a mutant form of Bcl6 lacking the ability to bind the corepressor NCOR also exhibited markedly diminished GC formation, whereas Tfh generation appeared intact (Huang et al., 2013). These studies emphasize the exquisite functional impact of individual components of Bcl6 transcriptional complexes at different genes or in different lineages.

The derepression of *Bcl6* and *Batf* occurred in the thymus and, in the case of *Batf*, was clearly associated with an increase in active epigenetic marks. Although a broader analysis of epigenetic changes should reveal the biochemical details and the extent of the Bcl6–Cul3-mediated repression program in thymocytes, the current results provide a simple explanation for the increased basal overexpression of these key Tfh-inducing genes detected first at the mRNA level in thymocytes, and then at the protein level around the time of emigration. Flow cytometric analysis of Batf and Bcl6 demonstrated that these changes were widespread at the single-cell level as shown by the global shifts of FACS profiles and therefore seemed sufficient to explain the long-range effect in mature peripheral $CD4^+$ T cells and their exaggerated induction of Batf and Bcl6 upon antigen stimulation. However, because ablation of Cul3 directly in mature post-thymic T cells also resulted in sustained Tfh responses, indicating that the negative autoregulatory feedback operated also during the peripheral activation of mature $CD4^+$ T cells, it remains unclear whether the thymic-stage alterations alone are sufficient to deregulate Tfh responses.

There is increasing understanding that Tfh responses are exquisitely regulated at multiple levels and through separate mechanisms. For example, previous studies have highlighted the relevance of TCR signal strength during antigen stimulation (Fazilleau et al., 2009; Deenick et al., 2010; Tubo et al., 2013). Another level of regulation of Tfh responses is mediated by the E3 ligases roquin 1 and 2, which act independently of Bcl6 and directly bind *Icos* mRNA to regulate its degradation (Vinuesa et al., 2005; Glasmacher et al., 2010; Pratama et al., 2013; Vogel et al., 2013). In contrast with these reported mechanisms, our study showed that the regulation of Tfh-inducing genes by Cul3 was independent of TCR signal strength and occurred directly at the level of Batf and Bcl6 transcription.

The Tfh expansion of Cul3cKO mice was conspicuously localized to mucosal draining lymph nodes and spleen and was not associated with the florid signs of systemic autoimmunity reported in *san/san* mice. This difference might suggest the presence of additional defects in *san/san* and roquin-deficient T cells (Pratama et al., 2013). Alternatively, associated B cell defects might be required to produce anti-DNA antibodies, as suggested by the absence of systemic autoimmunity in mice lacking roquin 1 and 2 selectively in their T cell department (Vogel et al., 2013). Rather than autoimmunity, a key role for environmental antigens is suggested by the mucosal distribution of the Tfh expansion in Cul3cKO mice and the requirement for antigen stimulation implied by the TCR Tg experiments. Future studies will address the role that microbiota and dietary antigens might play in these immune responses.

Bcl6-deficient mice were initially reported to exhibit poor health and eosinophilic infiltration of heart and lung, with Th2 skewing of their responses to environmental and experimental antigens (Dent et al., 1997; Ye et al., 1997). This dysregulation likely results from the combination of cell-intrinsic defects in several of the cell types in which Bcl6 is expressed, including macrophages, T cells, and B cells (Kusam et al., 2003; Mondal et al., 2010; Barish et al., 2012; Hollister et al., 2013). Unlike

Published May 26, 2014

Cul3cKO mice, Bcl6cKO mice did not exhibit Tfh expansion because this process requires Bcl6 itself, but their $CD4^+$ SP thymocytes did exhibit elevated basal levels of Batf, which, in conjunction with Irf4, can bind and activate many T helper effector genes (Ciofani et al., 2012; Glasmacher et al., 2012; Li et al., 2012; Tussiwand et al., 2012). In the absence of Bcl6, these derepressed factors might promote aberrant T helper effector responses that cause inflammatory pathology.

In conclusion, our findings reveal the role of Cul3 in the transcriptional repression of key Tfh-inducing genes by Bcl6, identifying a negative autoregulatory loop that is critical for limiting Tfh responses. This negative regulation operates when mature $CD4^+$ T cells develop Tfh responses in response to antigen in the periphery, but also during thymic development where the transient expression of Bcl6 appears to imprint multiple Tfh genes before thymocyte maturation and export.

MATERIALS AND METHODS

Mice. C57BL/6, B6.SJL-Ptprca Pep3b/BoyJ (CD45.1), and Cd4-Cre (B6 Tg(cd4-cre)1Cwi) mice were obtained from the Jackson Laboratory. MHC $II^{-/-}$ (I-$A\beta^{b-/-}$), MHC $I^{-/-}$ (β2microglobulin$^{-/-}$), and MHC $I/II^{-/-}$ mice in B6 background were purchased from Taconic. Sh2d1a $(SAP)^{-/-}$ (Wu et al., 2001) and $Cul3^{fl/fl}$ mice (McEvoy et al., 2007) in a B6 background were bred in our colony. We used $Cre^-Cul3^{fl/fl}$ mice as controls for Cul3cKO and OTII $Cre^-Cul3^{fl/fl}$ as controls for OTII Cul3cKO. $Bcl6^{fl/fl}$ mice have been described previously (Hollister et al., 2013). All mice were raised in a specific pathogen–free environment at the University of Chicago, and experiments were performed in accordance with the guidelines of the Institutional Animal Care and Use Committee.

Cell culture. HeLa cells were maintained in DMEM (Gibco) plus 10% FBS, 1% penicillin/streptomycin. All of the cell lines were initially purchased from the ATCC.

Bcl6 and Cul3 plasmids and antibodies. Human pcDNA3-myc-Cul3 and pcDNA3-myc-$Cul3^{mut}$ (L52AE55A) were previously described (Mathew et al., 2012). pcDNA3-Bcl6 was provided by B. Baron (University of Chicago, Chicago, IL). Anti-Myc (71D10 from Cell Signaling Technology or 9E10 from EMD Millipore) and anti-Bcl6 (Santa Cruz Biotechnology, Inc.) were used to stain confocal microscopy slides as described previously (Mathew et al., 2012).

Western blot analysis. 20×10^6 thymic DP or $CD4^+$ SP from B6 mice were lysed and immunoprecipitated with anti-Cul3 antibody (C-0871; Sigma-Aldrich) and Western blotted with anti-Bcl6 (BD), anti–c-Krox (Abcam), anti-Bach2 (Novus Biologicals), and anti-Cul3 (Singer et al., 1999).

Flow cytometry. Fluorochrome-labeled monoclonal antibodies against CD4 (GK1.5), CD8a (53-6.7), TCRβ (H57-597), CD44 (IM7), CD25 (PC61), B220 (RA3-6B2), CXCR5 (2G8), PD1 (29F.1A12, J43), ICOS (C398.4A), Fas (JO2), GL7 (GL7), CD3e (17A2), CD45.1 (A20), CD45.2 (104), CD19 (ID3), IgD (11-26c.2a), CD69 (H1.2F3), $\gamma\delta$-TCR (GL3), Vα2 (B20.1), Vβ5 (MR9-4), CXCR5 (L138D7), BTLA (HMBT-6B2), and OX40 (OX86) were purchased from e-Bioscience, BD, or BioLegend. We used either fluorophore-conjugated CXCR5 antibody (L138D7) or purified CXCR5 (2G8) antibody. For CXCR5 staining using purified antibody, cells were first incubated with 5 µg/ml of purified anti-CXCR5 (2G8; BD), followed by biotinylated Affini-Pure anti–rat IgG (Jackson ImmunoResearch Laboratories, Inc.) and APC-streptavidin (Invitrogen). After addition of 100 µg/ml of purified rat IgG2a isotype, cells were incubated with other extracellular antibodies. Bcl6 (clone K12-91; BD), Batf (clone MBM7C7; eBioscience), Foxp3 (clone FJK-16s; eBioscience), Tbet (clone 4B10; BioLegend), Ki-67 (clone SolA15; eBioscience), and Gata3 (TWAJ; eBioscience) were stained after fixation and permeabilization with the Foxp3 staining buffer set from eBioscience. Samples were analyzed on an LSRII (BD) or sorted on a FACSAria (BD) or MoFlo (Dako). Data were analyzed using FlowJo software (Tree Star).

Generation of bone marrow chimeras. 6–8-wk-old B6 (CD45.1 or CD45.1/CD45.2) mice were irradiated (100 Gy) using a gamma cell 40 irradiator with a cesium source and i.v. injected with $2–5 \times 10^6$ bone marrow cells from donor mice after T cell depletion using anti-CD3 and AutoMACS (Miltenyi Biotec). The recipient mice were analyzed 8–10 wk after irradiation.

Antinuclear antibodies. Serum dilutions were incubated with Hep-2 cells (AN-1012; MBL International), followed by FITC-conjugated anti–mouse IgG (eBioscience). Mean nuclear fluorescence intensities of 20 cells per sample were recorded using ImageJ software (National Institutes of Health). Positive control included a serum from $MRL^{lpr/lpr}$ mice.

OTII cell stimulation. For in vitro OTII cell stimulation, thymocytes were depleted of $CD69^+$ cells using PE-conjugated anti-CD69 and anti-PE magnetic microbeads followed by AutoMACS. 5×10^4 CD69-depleted thymocytes were incubated with 5×10^5 CD3-depleted CD45 congenic splenocytes and cultured with a range of OVAp (323–339) concentrations (GenScript) in duplicate in 96-microwell plates for 20 h at 37°C before FACS analysis. For in vivo cell transfer experiments, 5×10^5 CD8-depleted thymocytes from OTII or OTII Cul3cKO mice were i.v. transferred into CD45 congenic recipient mice 1 d before i.p. injection of 50 µg OVA (Worthington Biochemical Corporation) mixed 1:1 with alum (Thermo Fisher Scientific) or s.c. injection in the left and right hock of a total of 50 µg OVA mixed 1:1 with CFA (Sigma-Aldrich). Each mouse was injected s.c. in the left and right hind hock with 50 µl of the CFA emulsion containing 25 µg of OVA protein. OTII cells in recipient spleens were characterized by FACS after identification based on anti-CD45 allele-specific antibodies, anti-Vβ5 and anti-Vα2 antibodies.

Tfh-dependent antibody response to NP hapten. To measure the T helper–dependent antibody response to the hapten NP, 5×10^5 CD8-depleted thymocytes from OTII or OTII Cul3cKO mice were i.v. transferred into CD45.1/CD45.2 congenic recipient mice 1 d before i.p. immunization with 50 µg OVA-NP_{16} (Biosearch Technologies) mixed 1:1 with alum. Serum was collected 0 and 21 d later to titer anti-NP antibodies by ELISA against BSA-NP_{41} or BSA-NP_4 (Biosearch Technologies) coated on 96-well plates, using anti-IgG1 isotype-specific antibodies (BD). Values between different experiments were normalized to the same serum standard.

RTE assay. 6–8-wk-old mice were injected with 5 µl of a 1 mg/ml solution of FITC (Sigma-Aldrich) into each thymic lobe under anesthesia and killed 20 h later for analysis of $FITC^+$ spleen cells.

Retroviral infection. MIGR1 or MIGR1-Cre (Pear et al., 1998) was transfected into Plat-E cells, and viral supernatants were collected 48 and 72 h later. Splenic $CD4^+$ cells were enriched by MACS depletion with a mixture of anti-B220, -CD19, -Ter119, and -CD8a and stimulated with plate-bound anti-CD3 (5 µg/ml) and anti-CD28 (2 µg/ml) for 24 h before infection with viral supernatant (1 ml for 10^6 cells) in the presence of 5 µg/ml polybrene by spin infection for 90 min at 800 *g*. After transduction, 10^6 cells were injected i.v. into CD45 congenic mice, followed by i.p. immunization 24 h later with 50 µg OVA in alum (1:1).

Transient transfection of HeLa cells. HeLa cells were transfected using Lipofectamine (Invitrogen) as per the manufacturer's instruction with 0.5 µg Bcl6 and 2 µg Cul3 plasmids. Cells were harvested 24 h after transfection for confocal microscopy.

qRT-PCR. For qRT–PCR, total RNA was prepared from 10^6 sorted thymic $CD4^+$ SP ($CD4^+CD8^-TCR\gamma\delta^-CD25^-CD1d$–$\alpha$GalCer tetramer$^-$), large DP ($CD71^+FSC^{hi}$) or small DP ($CD71^-FSC^{lo}$) cells from Cul3cKO or Bcl6cKO, and their littermate controls by using TRIzol (Invitrogen), the RNeasy kit (QIAGEN), and reverse transcription with the Superscript III

first strand synthesis super mix cDNA kit (Invitrogen). cDNA expression was determined with the Mx3005P using Brilliant SYBR green master mix (Agilent Technologies). Fluorescence signals were measured over 40 PCR cycles, and the cycle (*Ct*) at which signals crossed a threshold set within the logarithmic phase was recorded. The *Ct* for the target gene was subtracted from the *Ct* for 18S (ΔCt), and $\Delta\Delta Ct$ was calculated by subtracting ΔCt for KO from ΔCt for littermate ($\Delta\Delta Ct$). The fold change of mRNA in KO over littermate was calculated as $2^{-\Delta\Delta Ct}$.

ChIP-qPCR. ChIP experiments were performed as previously described (Mathew et al., 2012). In brief, cells were fixed and isolated nuclei were resuspended in 130 µl nuclei lysis buffer (50 mM Tris-HCl, pH 8.1, 10 mM EDTA, 0.5% SDS, and 1× protease inhibitor) sonicated to obtain 100–500-bp fragments (Covaris-S220). Chromatin from 20 million cells was used for immunoprecipitation using anti-Bcl6 (sc-N3), anti-H3K4me3 (07-473; EMD Millipore), or anti-H3Ac (06-599; EMD Millipore). Specific DNA sequences were assessed by qRT-PCR using primers as listed.

qRT-PCR primers. The following qRT-PCR primers were used: *batf*_f, 5′-ACAGACACAGAAAGCCGACAC-3′; *batf*_r, 5′-CTCGGTGAGCTGTTTGATCTC-3′; *bcl6*_f, 5′-ACTGGGCAAACACAACATGG-3′; *bcl6*_r, 5′-GGAGGCGATTAAGGTTGAGAAG-3′; *bcl6*_exon 2–3_f, 5′-ACTGGGCAAACACAACATGG-3′; *bcl6*_exon 2–3_r, 5′-GGAGGCGATTAAGGTTGAGAAG-3′; *il21*_f, 5′-GCCAAACTCAAGCCATCAAACC-3′; *il21*_r, 5′-TTCTCATACGAATCACAGGAAGGG-3′; *c-maf*_f, 5′-AGCAGTTGGTGACCATGTCG-3′; *c-maf*_r, 5′-TGGAGATCTCCTGCTTGAGG-3′; 18s_f, 5′-TTGACTCAACACGGGAAACC-3′; 18s_r, 5′-ACCCACGGAATCGAGAAAGA-3′; *gapdh*_f, 5′-CTGGAGAAACCTGCCAAGTATG-3′; and *gapdh*_r, 5′-TCCTCAGTGTAGCCCAAGATG-3′.

Bcl6 ChIP-qPCR primers. The following Blc6 ChIP-qPCR primers were used: *bcl6*-f, 5′-GGGTTCTTAGAAGTGGTGATGC-3′; *bcl6*-r, 5′-CAGCAACAGCAATAATCACCTG-3′; *batf*-f, 5′-CGTCTCTGCCACTTAGGTTCC-3′; *batf*_r, 5′-TGGAACATTCCTCTGCTTATGG-3′; *bcl2*-f, 5′-TCTGCCCTGGAGGTCTGAAG-3′; *bcl2*-r, 5′-CTGTGATTCTCCCTTCTTCTCG-3′; *prdm1*-f, 5′-TGCAGAACTTCTAGGTTCTTTCTTG-3′; and *prdm1*-r, 5′-GCTTTGGAAGGTTCTGAATGG-3′.

Histone ChIP-qPCR primers. The following histone ChIP-qPCR primers were used: *batf*(−100)-f, 5′-TCGCTCTGCCTTTCAAACTG-3′; *batf*(−100)-r, 5′-AAGTCACATGGGCGGAAAC-3′; *batf*(+580bp)-f, 5′-CGTCTCTGCCACTTAGGTTCC-3′; *batf*(+580bp)-r, 5′-TGGAACATTCCTCTGCTTATGG-3′; *batf*(+700bp)-f, 5′-TGTTCCAGTAGATCGCTGCTTC-3′; *batf*(+700bp)-r, 5′-TCTGTCTTGCCACTTGCTTG-3′; *batf*(+1.5kb)-f, 5′-TTGCCCTCTCTAACCCAATG-3′; *batf*(+1.5kb)-r, 5′-CTTGGGTCAGGTTCTGATTCC-3′; *batf*(+2k)-f, 5′-AACGCGCTTGTACAGAAGTTG-3′; *batf*(+2k)-r, 5′-TGCGCACATGCTAAACCTTC-3′; *batf*(+2.5k)-f, 5′-CCTCCTGAGGCTTCAATTTCTC-3′; *batf*(+2.5k)-r, 5′-TCTTCAGCATTCCCTGCTACC-3′; *batf*(+3k)-f, 5′-CAGGTTGTGGAAAGGGCTTC-3′; *batf*(+3k)-r, 5′-AGAAAGGTTCAGTGTCCAGTGC-3′; *batf*(+3.5k)-f, 5′-TCATCGCATCCTTCTTCCTG-3′; *batf*(+3.5k)-r, 5′-CTTATCTGGGTTTGGCACCTC-3′; *batf*(+4k)-f, 5′-TCACACACGCATGTGCATC-3′; *batf*(+4k)-r, 5′-TATGTGCGTGTGGTGTTTCC-3′; *batf*(+9.5k)-f, 5′-ATGTCTGCGAGGCTGAATTG-3′; *batf*(+9.5k)-r, 5′-CCACCATTGGTAATTTGGAGAC-3′; *batf*(+18.5k)-f, 5′-TGATGGGCCTAACCACATTC-3′; *batf*(+18.5k)-r, 5′-TAGGCAGTGTGGAGATCAAGC-3′; *batf*(+18.8k)-f, 5′-TCCGAGCTTACAGACATTCCTC-3′; *batf*(+18.8k)-r, 5′-TGACTAACCACTGCCTGCTG-3′; *batf*(+19.4k)-f, 5′-AGCATTCAAAGTGTCGCTGAG-3′; *batf*(+19.4k)-r, 5′-TTAAGTTGTGGAGGAGCAGAGG-3′; *batf*(+20k)-f, 5′-CAAGCTTCTGGCCTGAAATG-3′; and *batf*(+20k)-r, 5′-CCCGGACCTGAATAAACAGAAC-3′.

Reporter assay. The proximal promoter, first exon, and first intron containing the Bcl6-binding motif of mouse *Batf* (−572 to 924) were cloned into the SmaI and XhoI site of pGL3-basic vector (Promega). To disrupt the Bcl6-binding site, a site-directed mutagenesis kit (Agilent Technologies) was used to change the sequences from 5′-TTTCTAGGAA-3′ (576/585: Bcl6_1) and 5′-TTTCCAGGAA-3′ (696/705: Bcl6_2) to 5′-TTGTCGACTA-3′ (m1) and 5′-TTGATATCGAC-3′ (m2), respectively. These plasmids were transfected along with a cmv-Renilla plasmid into 293T cells (ATCC) using Lipofectamine (Invitrogen). Reporter assays were performed using the dual luciferase detection system (Promega), and firefly luciferase levels were normalized to Renilla luciferase values.

Microarray analysis, strictly standardized mean difference (SSMD), and Monte Carlo analysis. RNA was isolated from FACS-sorted thymic $CD4^+$ SP cells ($CD4^+CD8^-TCR\gamma\delta^-CD25^-CD1d$–αGalCer tetramer$^-$) from 4.5-wk-old Cul3cKO and littermate controls using TRIzol and processed for 430A.v2 arrays (Affymetrix) according to the manufacturer's instructions. To test whether Tfh-related genes were non-randomly up-regulated in Cul3cKO thymocytes, we compared the SSMDs of Tfh-, Th1-, and Th2-related genes with the SSMDs of randomly generated subsets of genes. First, we selected Tfh-related genes (*Slamf6*, *Il21*, *Cxcr5*, *Maf*, *Icos*, *Irf4*, *Batf*, *Bcl6*, *Pdcd1*, *Sh2d1a*, *Tiam1*, *Stat4*, *Tnfsf11*, and *CD44*), Th1 genes (*Eomes*, *Tbet*, *Fasl*, *IL12rb2*, *Ifng*, *IL18rap*, *Stat1*, *Stat4*, *IL27ra*, *IL18r1*, *Cxcr3*, *Zbtb32*, and *Ccr5*), and Th2 genes (*pparg*, *Il5*, *Ccr1*, *Il1rl1*, *Areg*, *Il13*, *Il4*, *Gata3*, *Ccr3*, *Il13ra1*, *Il24*, *Ccr8*, *Ccr4*, *Stat6*, *IL4ra*, *Ccl5*, *Il9*, and *Ccl11*) based on previously published work (Vinuesa et al., 2005; Nurieva et al., 2008; Yusuf et al., 2010). Then, drawing from all genes represented on the microarray, we generated 10 million randomly selected, equally sized subsets of genes using the Monte Carlo method, producing an ensemble of gene sets to serve as a null distribution of possible observed effects. For each set of genes, we compared probe set intensities between Cul3 KO mice and their WT littermates, quantifying the overall effect size using a paired-sample SSMD (Zhang, 2011). The SSMD for paired observations is defined as the mean of the log fold changes (FC) divided by the standard deviation of the log fold changes:

$$\mathrm{SSMD} = \frac{\mu(\mathrm{FC}_1, \mathrm{FC}_2, ..., \mathrm{FC}_n)}{\sigma(\mathrm{FC}_1, \mathrm{FC}_2, ..., \mathrm{FC}_n)}.$$

FC_n denotes the log fold change for the *n*-th observation with respect to a negative reference, μ is the arithmetic mean, and σ is the standard deviation. The SSMD of the Tfh-related probe sets estimates the effect size of Cul3 deficiency on Tfh-specific genes, whereas the SSMDs for the randomly generated sets approximate the distribution of possible effects observed by chance alone. To estimate the statistical significance of Tfh-related gene up-regulation, we compared the SSMD of Tfh genes ($\mathrm{SSMD}_{\mathrm{Tfh}} = 0.788$) with the Monte Carlo–generated distribution of random SSMDs. In our sample of 10 million sets of genes, SSMDs greater than or equal to $\mathrm{SSMD}_{\mathrm{Tfh}}$ occurred 24 times, corresponding to a p-value of 2×10^{-6}. A similar analysis conducted for the Th1 and Th2 gene sets showed nonsignificant p-values of 0.3 in each case.

Statistical analysis. Unpaired Student's *t* test was performed with Prism (GraphPad Software). *, $P < 0.05$; **, $P < 0.01$; ***, $P < 0.001$.

Accession number. Gene expression data are available at the Gene Expression Omnibus (GEO) database under accession no. GSE56514.

This work was supported by the Cancer Research Institute (R. Mathew), National Institutes of Health (NIH) grants RO1 GM106173 and AI038339 and the Howard Hughes Medical Institute (to A. Bendelac), the University of Chicago Digestive Diseases Research Core Center grant P30 DK42086 and NIH grant R21 AI099825 (to A.L. Dent), and NIH grant RO1 GM082940 (to J.D. Singer). A.H. Chiang and A.R. Dinner's effort is in part sponsored by the Defense Advanced Research Projects Agency (D12AP00023), and the content of the information does not necessarily reflect the position or the policy of the Government, and no official endorsement should be inferred.

The authors declare no competing financial interests.

Submitted: 29 October 2013
Accepted: 11 April 2014

Published May 26, 2014

REFERENCES

Barish, G.D., R.T. Yu, M. Karunasiri, C.B. Ocampo, J. Dixon, C. Benner, A.L. Dent, R.K. Tangirala, and R.M. Evans. 2010. Bcl-6 and NF-κB cistromes mediate opposing regulation of the innate immune response. *Genes Dev.* 24:2760–2765. http://dx.doi.org/10.1101/gad.1998010

Barish, G.D., R.T. Yu, M.S. Karunasiri, D. Becerra, J. Kim, T.W. Tseng, L.J. Tai, M. Leblanc, C. Diehl, L. Cerchietti, et al. 2012. The Bcl6-SMRT/NCoR cistrome represses inflammation to attenuate atherosclerosis. *Cell Metab.* 15:554–562. http://dx.doi.org/10.1016/j.cmet.2012.02.012

Basso, K., and R. Dalla-Favera. 2012. Roles of BCL6 in normal and transformed germinal center B cells. *Immunol. Rev.* 247:172–183. http://dx.doi.org/10.1111/j.1600-065X.2012.01112.x

Betz, B.C., K.L. Jordan-Williams, C. Wang, S.G. Kang, J. Liao, M.R. Logan, C.H. Kim, and E.J. Taparowsky. 2010. Batf coordinates multiple aspects of B and T cell function required for normal antibody responses. *J. Exp. Med.* 207:933–942. http://dx.doi.org/10.1084/jem.20091548

Choi, Y.S., R. Kageyama, D. Eto, T.C. Escobar, R.J. Johnston, L. Monticelli, C. Lao, and S. Crotty. 2011. ICOS receptor instructs T follicular helper cell versus effector cell differentiation via induction of the transcriptional repressor Bcl6. *Immunity.* 34:932–946. http://dx.doi.org/10.1016/j.immuni.2011.03.023

Ciofani, M., A. Madar, C. Galan, M. Sellars, K. Mace, F. Pauli, A. Agarwal, W. Huang, C.N. Parkurst, M. Muratet, et al. 2012. A validated regulatory network for Th17 cell specification. *Cell.* 151:289–303. http://dx.doi.org/10.1016/j.cell.2012.09.016

Crotty, S. 2011. Follicular helper CD4 T cells (TFH). *Annu. Rev. Immunol.* 29:621–663. http://dx.doi.org/10.1146/annurev-immunol-031210-101400

Deenick, E.K., A. Chan, C.S. Ma, D. Gatto, P.L. Schwartzberg, R. Brink, and S.G. Tangye. 2010. Follicular helper T cell differentiation requires continuous antigen presentation that is independent of unique B cell signaling. *Immunity.* 33:241–253. http://dx.doi.org/10.1016/j.immuni.2010.07.015

Dent, A.L., A.L. Shaffer, X. Yu, D. Allman, and L.M. Staudt. 1997. Control of inflammation, cytokine expression, and germinal center formation by BCL-6. *Science.* 276:589–592. http://dx.doi.org/10.1126/science.276.5312.589

Duda, D.M., D.C. Scott, M.F. Calabrese, E.S. Zimmerman, N. Zheng, and B.A. Schulman. 2011. Structural regulation of cullin-RING ubiquitin ligase complexes. *Curr. Opin. Struct. Biol.* 21:257–264. http://dx.doi.org/10.1016/j.sbi.2011.01.003

Errington, W.J., M.Q. Khan, S.A. Bueler, J.L. Rubinstein, A. Chakrabartty, and G.G. Privé. 2012. Adaptor protein self-assembly drives the control of a cullin-RING ubiquitin ligase. *Structure.* 20:1141–1153. http://dx.doi.org/10.1016/j.str.2012.04.009

Fazilleau, N., L.J. McHeyzer-Williams, H. Rosen, and M.G. McHeyzer-Williams. 2009. The function of follicular helper T cells is regulated by the strength of T cell antigen receptor binding. *Nat. Immunol.* 10:375–384. http://dx.doi.org/10.1038/ni.1704

Glasmacher, E., K.P. Hoefig, K.U. Vogel, N. Rath, L. Du, C. Wolf, E. Kremmer, X. Wang, and V. Heissmeyer. 2010. Roquin binds inducible costimulator mRNA and effectors of mRNA decay to induce microRNA-independent post-transcriptional repression. *Nat. Immunol.* 11:725–733. http://dx.doi.org/10.1038/ni.1902

Glasmacher, E., S. Agrawal, A.B. Chang, T.L. Murphy, W. Zeng, B. Vander Lugt, A.A. Khan, M. Ciofani, C.J. Spooner, S. Rutz, et al. 2012. A genomic regulatory element that directs assembly and function of immune-specific AP-1-IRF complexes. *Science.* 338:975–980. http://dx.doi.org/10.1126/science.1228309

Guo, J., A. Hawwari, H. Li, Z. Sun, S.K. Mahanta, D.R. Littman, M.S. Krangel, and Y.W. He. 2002. Regulation of the TCRα repertoire by the survival window of $CD4^+CD8^+$ thymocytes. *Nat. Immunol.* 3:469–476. http://dx.doi.org/10.1038/ni791

Hollister, K., S. Kusam, H. Wu, N. Clegg, A. Mondal, D.V. Sawant, and A.L. Dent. 2013. Insights into the role of Bcl6 in follicular Th cells using a new conditional mutant mouse model. *J. Immunol.* 191:3705–3711. http://dx.doi.org/10.4049/jimmunol.1300378

Huang, C., K. Hatzi, and A. Melnick. 2013. Lineage-specific functions of Bcl-6 in immunity and inflammation are mediated by distinct biochemical mechanisms. *Nat. Immunol.* 14:380–388. http://dx.doi.org/10.1038/ni.2543

Hyjek, E., A. Chadburn, Y.F. Liu, E. Cesarman, and D.M. Knowles. 2001. BCL-6 protein is expressed in precursor T-cell lymphoblastic lymphoma and in prenatal and postnatal thymus. *Blood.* 97:270–276. http://dx.doi.org/10.1182/blood.V97.1.270

Ise, W., M. Kohyama, B.U. Schraml, T. Zhang, B. Schwer, U. Basu, F.W. Alt, J. Tang, E.M. Oltz, T.L. Murphy, and K.M. Murphy. 2011. The transcription factor BATF controls the global regulators of class-switch recombination in both B cells and T cells. *Nat. Immunol.* 12:536–543. http://dx.doi.org/10.1038/ni.2037

Kusam, S., L.M. Toney, H. Sato, and A.L. Dent. 2003. Inhibition of Th2 differentiation and GATA-3 expression by BCL-6. *J. Immunol.* 170:2435–2441. http://dx.doi.org/10.4049/jimmunol.170.5.2435

Li, P., R. Spolski, W. Liao, L. Wang, T.L. Murphy, K.M. Murphy, and W.J. Leonard. 2012. BATF-JUN is critical for IRF4-mediated transcription in T cells. *Nature.* 490:543–546. http://dx.doi.org/10.1038/nature11530

Liu, X., R.I. Nurieva, and C. Dong. 2013. Transcriptional regulation of follicular T-helper (Tfh) cells. *Immunol. Rev.* 252:139–145. http://dx.doi.org/10.1111/imr.12040

Lu, K.T., Y. Kanno, J.L. Cannons, R. Handon, P. Bible, A.G. Elkahloun, S.M. Anderson, L. Wei, H. Sun, J.J. O'Shea, and P.L. Schwartzberg. 2011. Functional and epigenetic studies reveal multistep differentiation and plasticity of in vitro-generated and in vivo-derived follicular T helper cells. *Immunity.* 35:622–632. http://dx.doi.org/10.1016/j.immuni.2011.07.015

Mathew, R., M.P. Seiler, S.T. Scanlon, A.P. Mao, M.G. Constantinides, C. Bertozzi-Villa, J.D. Singer, and A. Bendelac. 2012. BTB-ZF factors recruit the E3 ligase cullin 3 to regulate lymphoid effector programs. *Nature.* 491:618–621. http://dx.doi.org/10.1038/nature11548

McEvoy, J.D., U. Kossatz, N. Malek, and J.D. Singer. 2007. Constitutive turnover of cyclin E by Cul3 maintains quiescence. *Mol. Cell. Biol.* 27:3651–3666. http://dx.doi.org/10.1128/MCB.00720-06

Mondal, A., D. Sawant, and A.L. Dent. 2010. Transcriptional repressor BCL6 controls Th17 responses by controlling gene expression in both T cells and macrophages. *J. Immunol.* 184:4123–4132. http://dx.doi.org/10.4049/jimmunol.0901242

Nakayamada, S., Y. Kanno, H. Takahashi, D. Jankovic, K.T. Lu, T.A. Johnson, H.W. Sun, G. Vahedi, O. Hakim, R. Handon, et al. 2011. Early Th1 cell differentiation is marked by a Tfh cell-like transition. *Immunity.* 35:919–931. http://dx.doi.org/10.1016/j.immuni.2011.11.012

Nurieva, R.I., Y. Chung, D. Hwang, X.O. Yang, H.S. Kang, L. Ma, Y.H. Wang, S.S. Watowich, A.M. Jetten, Q. Tian, and C. Dong. 2008. Generation of T follicular helper cells is mediated by interleukin-21 but independent of T helper 1, 2, or 17 cell lineages. *Immunity.* 29:138–149. http://dx.doi.org/10.1016/j.immuni.2008.05.009

Nurieva, R.I., Y. Chung, G.J. Martinez, X.O. Yang, S. Tanaka, T.D. Matskevitch, Y.H. Wang, and C. Dong. 2009. Bcl6 mediates the development of T follicular helper cells. *Science.* 325:1001–1005. http://dx.doi.org/10.1126/science.1176676

Nutt, S.L., and D.M. Tarlinton. 2011. Germinal center B and follicular helper T cells: siblings, cousins or just good friends? *Nat. Immunol.* 12:472–477. http://dx.doi.org/10.1038/ni.2019

Parekh, S., J.M. Polo, R. Shaknovich, P. Juszczynski, P. Lev, S.M. Ranuncolo, Y. Yin, U. Klein, G. Cattoretti, R. Dalla Favera, et al. 2007. BCL6 programs lymphoma cells for survival and differentiation through distinct biochemical mechanisms. *Blood.* 110:2067–2074. http://dx.doi.org/10.1182/blood-2007-01-069575

Pasqualucci, L., A. Migliazza, K. Basso, J. Houldsworth, R.S. Chaganti, and R. Dalla-Favera. 2003. Mutations of the BCL6 proto-oncogene disrupt its negative autoregulation in diffuse large B-cell lymphoma. *Blood.* 101:2914–2923. http://dx.doi.org/10.1182/blood-2002-11-3387

Pear, W.S., J.P. Miller, L. Xu, J.C. Pui, B. Soffer, R.C. Quackenbush, A.M. Pendergast, R. Bronson, J.C. Aster, M.L. Scott, and D. Baltimore. 1998. Efficient and rapid induction of a chronic myelogenous leukemia-like myeloproliferative disease in mice receiving P210 bcr/abl-transduced bone marrow. *Blood.* 92:3780–3792.

Pepper, M., A.J. Pagán, B.Z. Igyártó, J.J. Taylor, and M.K. Jenkins. 2011. Opposing signals from the Bcl6 transcription factor and the interleukin-2 receptor generate T helper 1 central and effector memory cells. *Immunity.* 35:583–595. http://dx.doi.org/10.1016/j.immuni.2011.09.009

Pratama, A., R.R. Ramiscal, D.G. Silva, S.K. Das, V. Athanasopoulos, J. Fitch, N.K. Botelho, P.P. Chang, X. Hu, J.J. Hogan, et al. 2013. Roquin-2 shares functions with its paralog Roquin-1 in the repression of mRNAs controlling T follicular helper cells and systemic inflammation. *Immunity*. 38:669–680. http://dx.doi.org/10.1016/j.immuni.2013.01.011

Schraml, B.U., K. Hildner, W. Ise, W.L. Lee, W.A. Smith, B. Solomon, G. Sahota, J. Sim, R. Mukasa, S. Cemerski, et al. 2009. The AP-1 transcription factor Batf controls T_H17 differentiation. *Nature*. 460:405–409.

Singer, J.D., M. Gurian-West, B. Clurman, and J.M. Roberts. 1999. Cullin-3 targets cyclin E for ubiquitination and controls S phase in mammalian cells. *Genes Dev.* 13:2375–2387. http://dx.doi.org/10.1101/gad.13.18.2375

Sun, Z., D. Unutmaz, Y.R. Zou, M.J. Sunshine, A. Pierani, S. Brenner-Morton, R.E. Mebius, and D.R. Littman. 2000. Requirement for RORγ in thymocyte survival and lymphoid organ development. *Science*. 288:2369–2373. http://dx.doi.org/10.1126/science.288.5475.2369

Tubo, N.J., A.J. Pagán, J.J. Taylor, R.W. Nelson, J.L. Linehan, J.M. Ertelt, E.S. Huseby, S.S. Way, and M.K. Jenkins. 2013. Single naive $CD4^+$ T cells from a diverse repertoire produce different effector cell types during infection. *Cell*. 153:785–796. http://dx.doi.org/10.1016/j.cell.2013.04.007

Tussiwand, R., W.L. Lee, T.L. Murphy, M. Mashayekhi, W. K C, J.C. Albring, A.T. Satpathy, J.A. Rotondo, B.T. Edelson, N.M. Kretzer, et al. 2012. Compensatory dendritic cell development mediated by BATF-IRF interactions. *Nature*. 490:502–507. http://dx.doi.org/10.1038/nature11531

Vinuesa, C.G., and J.G. Cyster. 2011. How T cells earn the follicular rite of passage. *Immunity*. 35:671–680. http://dx.doi.org/10.1016/j.immuni.2011.11.001

Vinuesa, C.G., M.C. Cook, C. Angelucci, V. Athanasopoulos, L. Rui, K.M. Hill, D. Yu, H. Domaschenz, B. Whittle, T. Lambe, et al. 2005. A RING-type ubiquitin ligase family member required to repress follicular helper T cells and autoimmunity. *Nature*. 435:452–458. http://dx.doi.org/10.1038/nature03555

Vogel, K.U., S.L. Edelmann, K.M. Jeltsch, A. Bertossi, K. Heger, G.A. Heinz, J. Zöller, S.C. Warth, K.P. Hoefig, C. Lohs, et al. 2013. Roquin paralogs 1 and 2 redundantly repress the Icos and Ox40 costimulator mRNAs and control follicular helper T cell differentiation. *Immunity*. 38:655–668. http://dx.doi.org/10.1016/j.immuni.2012.12.004

Wang, X., Z. Li, A. Naganuma, and B.H. Ye. 2002. Negative autoregulation of BCL-6 is bypassed by genetic alterations in diffuse large B cell lymphomas. *Proc. Natl. Acad. Sci. USA*. 99:15018–15023. http://dx.doi.org/10.1073/pnas.232581199

Wimuttisuk, W., and J.D. Singer. 2007. The Cullin3 ubiquitin ligase functions as a Nedd8-bound heterodimer. *Mol. Biol. Cell*. 18:899–909. http://dx.doi.org/10.1091/mbc.E06-06-0542

Wu, C., K.B. Nguyen, G.C. Pien, N. Wang, C. Gullo, D. Howie, M.R. Sosa, M.J. Edwards, P. Borrow, A.R. Satoskar, et al. 2001. SAP controls T cell responses to virus and terminal differentiation of TH2 cells. *Nat. Immunol.* 2:410–414. http://dx.doi.org/10.1038/87713

Ye, B.H., G. Cattoretti, Q. Shen, J. Zhang, N. Hawe, R. de Waard, C. Leung, M. Nouri-Shirazi, A. Orazi, R.S. Chaganti, et al. 1997. The BCL-6 proto-oncogene controls germinal-centre formation and Th2-type inflammation. *Nat. Genet*. 16:161–170. http://dx.doi.org/10.1038/ng0697-161

Yu, D., S. Rao, L.M. Tsai, S.K. Lee, Y. He, E.L. Sutcliffe, M. Srivastava, M. Linterman, L. Zheng, N. Simpson, et al. 2009. The transcriptional repressor Bcl-6 directs T follicular helper cell lineage commitment. *Immunity*. 31:457–468. http://dx.doi.org/10.1016/j.immuni.2009.07.002

Yusuf, I., R. Kageyama, L. Monticelli, R.J. Johnston, D. Ditoro, K. Hansen, B. Barnett, and S. Crotty. 2010. Germinal center T follicular helper cell IL-4 production is dependent on signaling lymphocytic activation molecule receptor (CD150). *J. Immunol.* 185:190–202. http://dx.doi.org/10.4049/jimmunol.0903505

Zhang, X.D. 2011. Illustration of SSMD, z score, SSMD*, z* score, and t statistic for hit selection in RNAi high-throughput screens. *J. Biomol. Screen*. 16:775–785. http://dx.doi.org/10.1177/1087057111405851